Average Characteristics and Activity Dependence of the Subauroral Polarization Stream

J. C. Foster and H. B. Vo
MIT Haystack Observatory, Westford, MA

Abstract

Data from the Millstone Hill incoherent scatter radar taken over two solar cycles (1979-2000) are examined to determine the average characteristics of the disturbance convection electric field in the midlatitude ionosphere. Radar azimuth scans provide a regular database of ionospheric plasma convection observations spanning auroral and subauroral latitudes, and these scans have been examined for all local times and activity conditions.We examine the occurrence and characteristics of a persistent secondary westward convection peak which lies equatorward of the auroral two-cell convection. Individual scans and average patterns of plasma flow identify and characterize this latitudinally-broad and persistent subauroral polarization stream (SAPS), which spans the nightside from dusk to the early morning sector for all Kp greater than 4. Pre-midnight, the SAPS westward convection lies equatorward of L = 4 (60˚ invariant latitude, Λ), spans 3˚ - 5˚ of latitude, and has an average peak amplitude of >900 m/s. In the pre-dawn sector, SAPS is seen as a region of antisunward convection equatorward of L = 3 (55˚ Λ), spanning ~3˚ of latitude, with an average peak amplitude of 400 m/s.

Introduction

During geomagnetic disturbances, the electric fields and particle populations which characterize the auroral region expand equatorward and their effects are felt at previously subauroral latitudes. Evidence of penetration of convection electric fields to mid latitudes has been presented in case studies using mid and low-latitude incoherent scatter radars (Wand and Evans, [1981], Gonzales et al, [1978], Yeh et al., [1991], Foster and Rich [1998]). These and similar studies have found in the night time sector enhanced convection which departs significantly from the standard Volland-Stern two-cell pattern [Stern, 1975; Volland, 1978]. From polar orbiting satellite observations, a polarization jet [Galperin et al., 1974] or SAID (subauroral ion drifts) [Smiddy et al., 1977; Spiro et al, 1979] is seen as westward convection with magnitude in excess of 500 m s^{-1}, equatorward of the auroral precipitation, and often associated with an ionospheric trough [Anderson et al., [1991]. SAID have been associated with disturbed conditions, and specifically with substorm recovery (Anderson et al., [1993], Karlsson et al, [1998]). Anderson et al., [2001] find SAID to be magnetically-conjugate, coherent features, associated with the conductivity distribution in the subauroral ionosphere and the midlatitude trough, and extending across local times from dusk to midnight. Anderson et al. [2001] provides a thorough overview of SAID observations and characteristics and a synopsis of the results of previous studies.

A more latitudinally-widespread disturbance-related region of subauroral electric field was reported by Yeh et al [1991], who described a second, broad region of westward plasma drift, equatorward and clearly separated from the usual dusk-sector two-cell auroral convection. The relationship of this subauroral region to particle and conductivity boundaries, and to the overlying ring current particle population, was described by those authors. Yeh et al [1991] found that the

low-latitude ion drift peak is closely related to the maximum of the O+ dominated ring current energy density. Burke et al. [1998] further describe the large potential difference and wide spatial extent across the subauroral electric field of such a region during a major geomagnetic storm.

In-situ electric field data further characterize this subauroral feature. One year of data from ISEE 1 was used by Maynard et al [1983] to determine the average characteristics of the electric field from L of 2 to 6. Those data indicated a penetration of the convection field into $L < 4$ during disturbed conditions in the late evening and early morning sector. Rowland and Wygant [1998] studied in situ electric field data from CRESS for a 10 month period in 1991 and showed the presence of a localized region of enhanced electric field between $L = 3$ and $L = 6$ for $Kp > 3$.

Global electric field models feature a dominant two-cell pattern of plasma convection whose equatorward portion transports ionospheric plasma sunward toward the noon meridian. The effects of plasma transport, and the linkage of the driving electric field to the overlying magnetosphere, dominate ionospheric characteristics at auroral and subauroral latitudes. With increasing activity level, and particularly during geomagnetic storms, the equatorward extent of such effects expands to lower latitudes [e.g., Foster et al., 1986; Weimer, 2001]. The empirical electric field model of Foster et al. [1986] demonstrates that the equatorward extent of the two-cell sunward convection is approximately coincident with the limit of plasma sheet particle precipitation. A common feature of many empirical convection models is a lack of measurements or of an extension of the model into the subauroral region equatorward of 55˚ invariant latitude (Λ). Such models do not accurately represent the inner magnetospheric convection electric field and its significant variation during disturbed conditions. It is important that the subauroral electric fields, as described in this and related papers dealing with the observations of this phenomenon, be included properly in models of ring current formation and stormtime ionosphere/thermosphere dynamics. To this end, we present here the average characteristics of the subauroral electric field derived from a database of Millstone Hill incoherent scatter radar observations which spans two solar cycles.

Foster and Burke [2002] introduced the term subauroral polarization stream (SAPS) to encompass both types of observations of subauroral electric fields, the SAID/polarization jet structures and the broader regions described by *Yeh et al.* [1991]. In this paper we use this term, SAPS, in our discussion of the statistical characteristics of this persistent region of poleward-directed electric field (westward plasma convection) at subauroral latitudes in the nightside magnetosphere-ionosphere system.

Radar Observations of Subauroral Ion Convection

The Massachusetts Institute of Technology maintains an extensive radar research facility at Millstone Hill, located 35 miles northwest of metropolitan Boston at 42.6˚ N latitude, 288.5˚ E longitude. Multi-megawatt UHF transmitters and a fully-steerable 46-m antenna provide wide-ranging spatial coverage, spanning >30˚ of latitude and 4+ hours of local time at *F* region heights with ~30-min temporal resolution. The facility is situated at 54˚Λ (L~3) such that its extensive field-of-view for ionospheric observations encompasses the full extent of mid-latitude, subauroral, and auroral features and processes. The Millstone Hill incoherent scatter radar has been in operation through three solar cycles (since 1979 using the steerable antenna) and its data characterize ionospheric features and response over the altitude range 100 km to 1000 km. Long-term operations as a part of the international Incoherent Scatter World Day program and during storm-alert experiments have built up a large database of azimuth scans across the sector from 220˚ to 350˚, which is centered on the magnetic L-shell aligned westward direction.

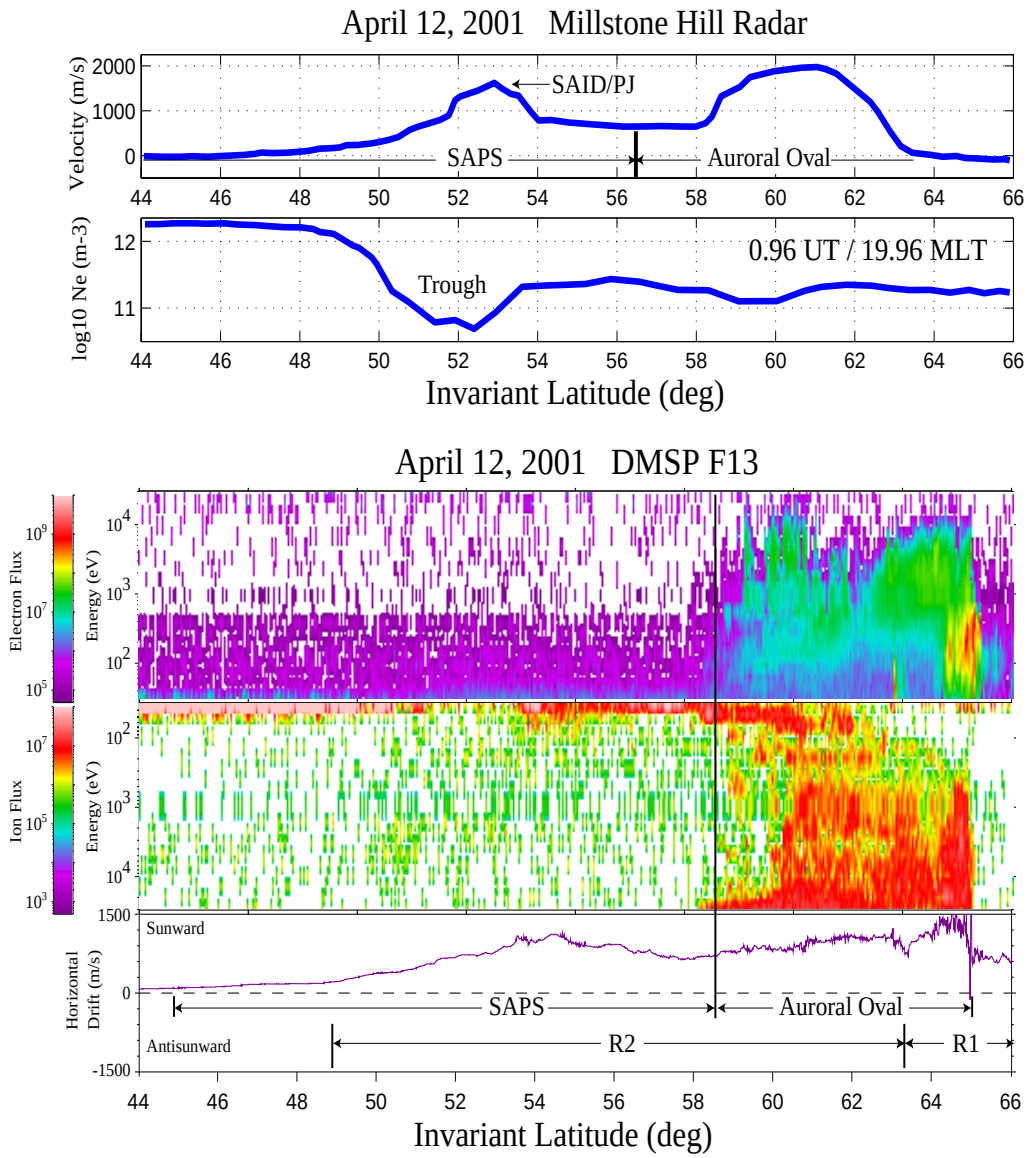

Figure 1. Millstone Hill ISR and simultaneous DMSP pass across the subauroral polarization stream at 20 MLT. SAPS appears as a region of strong westward ion velocity, equatorward of the auroral 2-cell convection and coincident with a deep ionospheric trough. Region 1 (R1) and Region 2 (R2) field aligned currents have been determined using the DMSP magnetometer (not shown). [after Foster and Burke, 2002].

The upper portion of Figure 1 presents latitude profiles of ionospheric convection and plasma density observed at 500 km altitude during a single Millstone Hill azimuth scan. Two distinct regions of sunward (westward) plasma convection are apparent, with the more-equatorward region coincident with a deep ionospheric trough. Data from a coincident DMSP F13 pass are shown below the radar data. Ion drift meter observations (bottom) repeat the double-peaked distribution of westward convection seen by the radar. The DMSP particle-flux observations (middle) clearly demonstrate that the more equatorward convection region lies entirely in the low-conductivity

region equatorward of the limit of plasma sheet particle precipitation. This subauroral polarization stream and deep F-region ionization trough lies within the region of the Region 2 (R2) field aligned currents identified with the DMSP magnetometer data (not shown) [Foster and Burke, 2002]. Yeh et al. [1991] described the occurrence of similar broad regions of subauroral westward convection and their relationship to particle and conductivity boundaries. In the case presented in Figure 1, the strength of the subauroral peak is comparable to that in the auroral pattern - both were near 1500 m/s - and the subauroral peak spans 5˚ of latitude. In the present study, we investigate the occurrence and characteristics of this secondary, subauroral plasma convection peak from a radar database of 9800 similar azimuth scans.

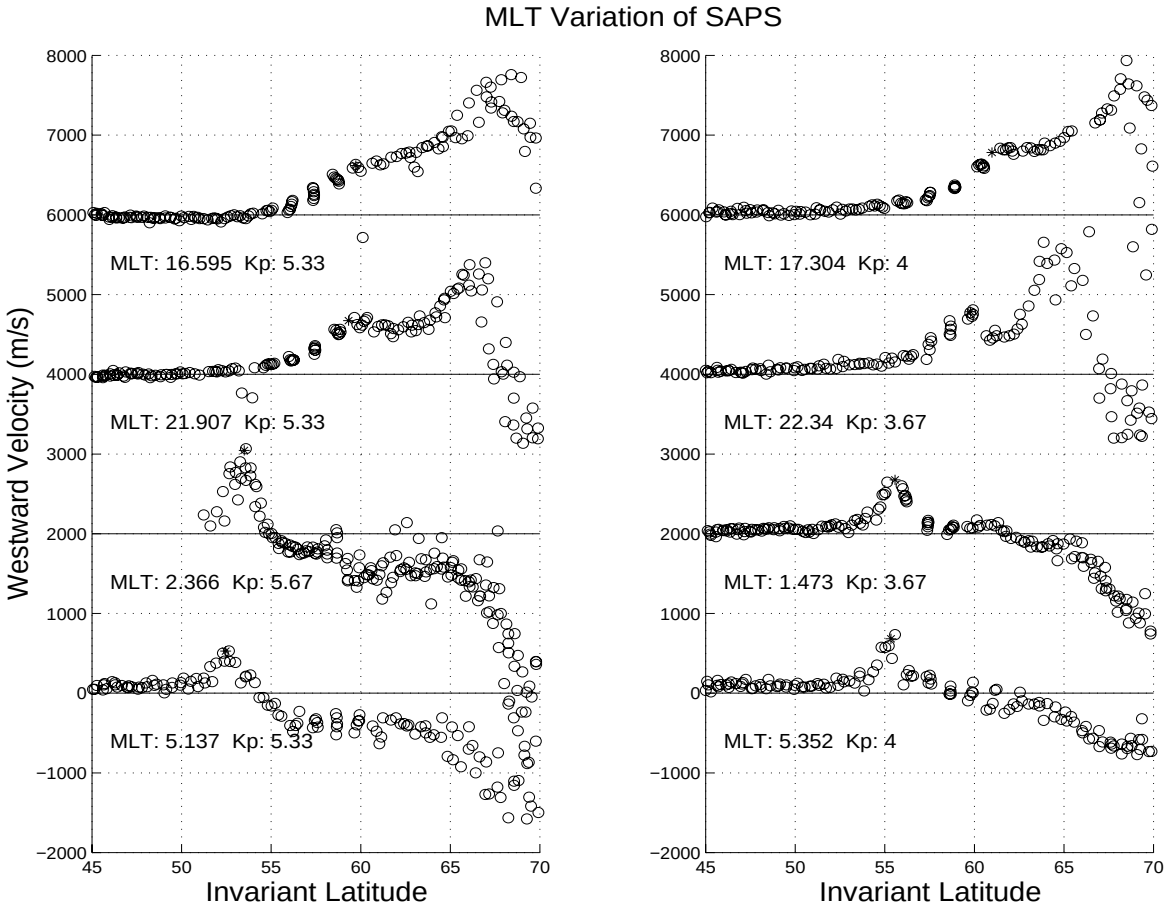

Figure 2. SAPS is seen as an activity-dependent, subauroral westward velocity peak which separates from the high-latitude two-cell convection near dusk and is observed across the midnight sector. Representative individual radar azimuth scans across the SAPS region are shown. Individual radar velocity samples are shown by open circles and our determination of the SAPS peak is indicated by "*".

Statistical Studies of the Subauroral Polarization Stream

Our statistical study addresses the broad region of poleward electric field and westward plasma convection found between the plasma sheet precipitation boundary and the conductivity

gradient at the plasmapause. This current-driven feature is closely associated with the region of low ionospheric conductance and with a source related to the formation of pressure gradients in the hot particle populations of the inner magnetosphere [cf. Vasyliunas, 1968; Yeh et al., 1991; Ridley and Liemohn, 2002]. Both SAID and polarization jets are intense, localized phenomena which occur within this larger region [Erickson et al., 2002].

Independent observations of line of sight plasma **ExB** velocity from all Millstone Hill azimuth scans over a 20-year interval were screened for bad data and were corrected with a magnetic direction cosine factor to yield the westward component of the flow. (Here we assume that the subauroral flow is basically L-shell aligned in the region of interest. The magnitude of the westward ion velocity is proportional to the poleward-directed component of the electric field in the *F* region.) Nearly 2 complete solar cycles of radar data (1978 to 2000) have been processed to yield a database of ~ 1.4 million ion velocity measurements for Kp > 2 conditions, each identified by date, magnetic latitude, local time, and activity level. Figure 2 presents representative plasma convection observations for local times from dusk through midnight to dawn and for two levels of Kp. SAPS convection is the more equatorward feature in each scan and can be seen separating from the higher-latitude two-cell convection peak as local time increases. (A similar result for SAID was reported by Anderson et al. [1991].) The separation of the two convection regions increases with increasing Kp as pointed out by Yeh et al. [1991] and Rowland and Wygant [1998]. Prominent in the observations of Figure 2 are the occurrences of strong westward convection (500 - 1000 m/s) near 55˚Λ (L~3) well into the post-midnight MLT sector. The occurrence of a pronounced westward anti-sunward convection feature equatorward of the dawn-sector two-cell pattern (cf. at 5.5 MLT in Figure 2) was reported by Huang et al. [2001] as due to the continuance of a ring current-induced convection feature (SAPS) into the morning sector. The statistical repeatability of the morning-sector feature is confirmed in the present study.

Characteristics of Individual SAPS Observations

We have examined each of the 9800 scans in the Millstone Hill database in order to identify and characterize the occurrence of SAPS. Each azimuth scan was displayed separately as shown in Figure 2 and the invariant latitude and amplitude of each SAPS feature was identified visually and recorded in a SAPS database for subsequent analysis. Asterisks on Figure 2 indicate the magnitude and position of the SAPS peaks identified for those scans. All scans for Kp > 2 were investigated and SAPS was identified in >1300 cases (occurrence statistics are treated below). Few occurrences can be found for Kp < 2 and there are very few occurrences in the sunlit sector between 08 MLT and 16 MLT.

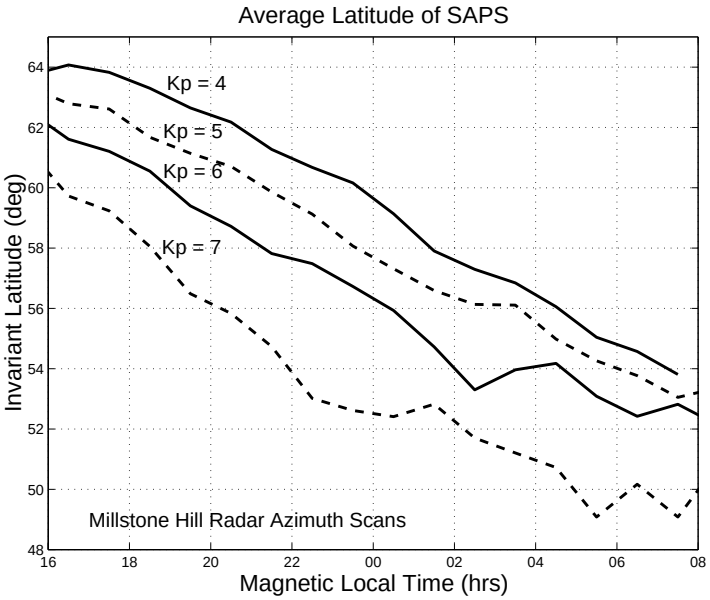

Figure 3. The average latitude of the peak of the polarization stream decreases uniformly as a function of both MLT and increasing Kp index.

A standard set of criteria were used in identifying the polarization stream convection velocity region in the radar scan data. For this study, SAPS was defined as a clearly identifiable region of westward ion convection velocity at or equatorward of the low-latitude edge of the auroral two-cell region. A SAPS peak is often separated from the auroral westward (pre-midnight) or eastward (post-midnight) two-cell region, or can be seen as an inflection-point enhancement on the equatorward slope of the dusk-sector two-cell region (cf. Figure 2, top panels at ~17 MLT). There is an element of subjectivity in the application of these criteria, but the method gives repeatable, consistent results.

Figure 3 presents the MLT variation of the mean latitude of the polarization stream for different Kp as determined using this peak-picking method. Mean latitude is seen to decrease linearly at a rate of ~0.7 deg per hour of local time. With increasing Kp, the SAPS region is shifted equatorward at all local times. SAPS occurs near 62˚Λ near dusk for Kp ~ 4, and near L = 3 (55˚Λ) at midnight, and at ~52˚Λ at dawn for high activity levels (standard deviations ~ 2˚ of latitude). The SAPS position in the post-midnight sector could be an ionospheric signature of the morning-sector plasmapause since both features tend to be associated with the poleward wall of the plasma density trough [Foster et al., 1978; Huang et al., 2001].

In order to characterize the width of the SAPS convection region, we have determined the equatorward and poleward limits of the SAPS westward convection region for each scan in the SAPS database in one-hour MLT windows centered at 22 MLT and 03 MLT. A threshold of >250 m/s was used for the pre-midnight scans and > 100 m/s for the post-midnight data. Premidnight, when the SAPS was not clearly separated from the auroral westward convection region, the inflection point separating the two regions was chosen as the poleward boundary. Figure 4 presents histograms of the individual SAPS widths so determined. The polarization stream spans 3˚ - 5˚ of invariant latitude at 22 MLT and ~ 3˚Λ at 03 MLT.

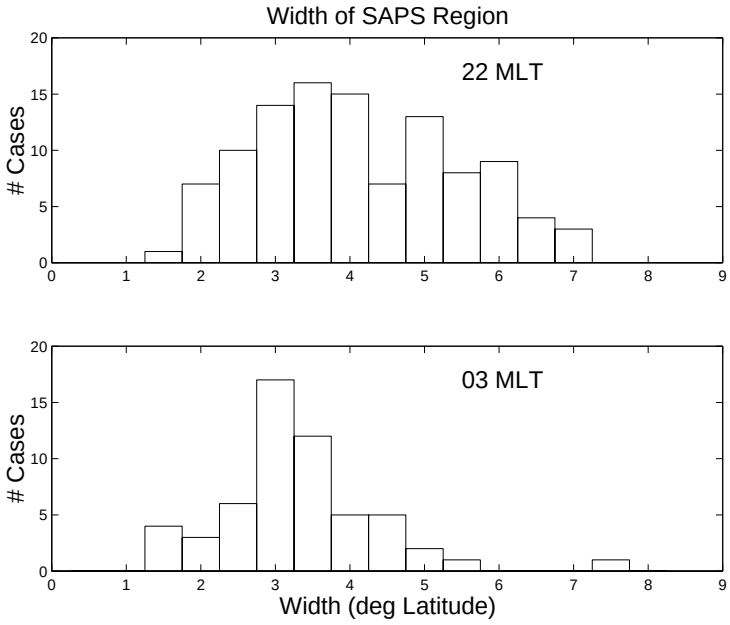

Figure 4. The latitudinal width of the polarization stream determined from the Millstone Hill radar scans is 3˚ - 5˚ in the pre-midnight sector and ~3˚ post-midnight.

The average magnitude of the peak SAPS ion velocity has been determined as a function of MLT across the nightside and for Kp values between 2 and 8. These results are presented in Figure 5 with a 250 m/s contour interval. The standard deviations of the averages in each MLT/Kp bin are clustered around ~275 m/s. Individual azimuth-scan velocity observations with the Millstone Hill incoherent scatter radar are 30-s volumetric averages of the ion bulk motion smeared over ~150 km along the radar beam pointing direction. Both fine-scale spatial and temporal structure in the sampling region are smoothed out in the sampling process. Maximum average velocity is found for Kp ~6 near 20 MLT (> 1000 m/s) and strong SAPS flows span the midnight sector between 18

MLT and 02 MLT for Kp 4 - 6. The intense subauroral SAID convection events reported by Karlsson et al. [1998] are strongest near 22 MLT and span the 18 MLT - 02 MLT sector.

Each radar scan in the SAPS database observed the SAPS peak at a specific latitude, and samples the overall latitude profile of plasma convection at the MLT and Kp of the scan. Figure 3 has presented the average latitude of the SAPS peak at each MLT and Kp. By superposing all SAPS peaks at the average latitude for a given MLT and Kp, we can investigate the spatial relationship of the SAPS region to the overall nightside ionospheric convection pattern. The results of such a superimposed binned modeling are presented in Figure 6 for Kp [5^+,6^0] conditions as a function of MLT and invariant latitude. The latitude/MLT variation of the average SAPS peak location is presented an a heavy solid line. For these conditions, SAPS is seen as strong westward convection (>500 m/s) equatorward

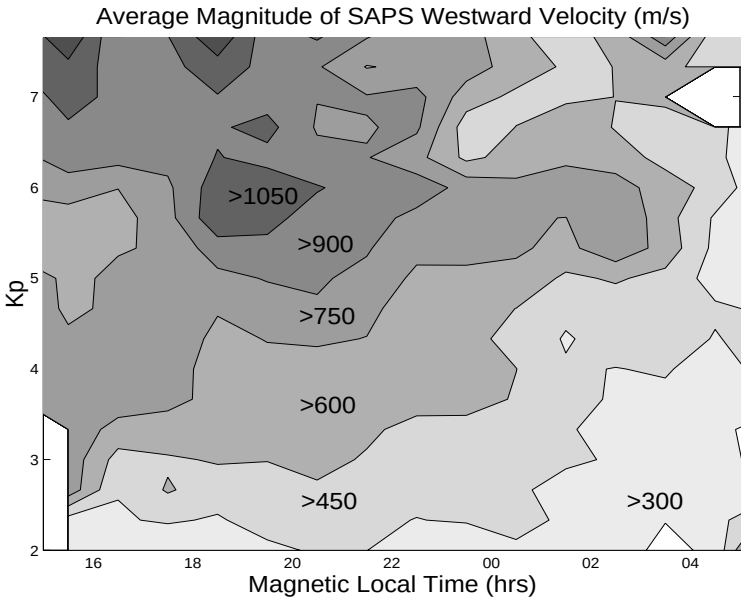

Figure 5.The average magnitude of the peak SAPS westward velocity observed from Millstone Hill has been determined as a function of Kp and MLT. The average SAPS peak velocity exceeds 1000 m/s near 20 MLT for Kp ~ 6 conditions.

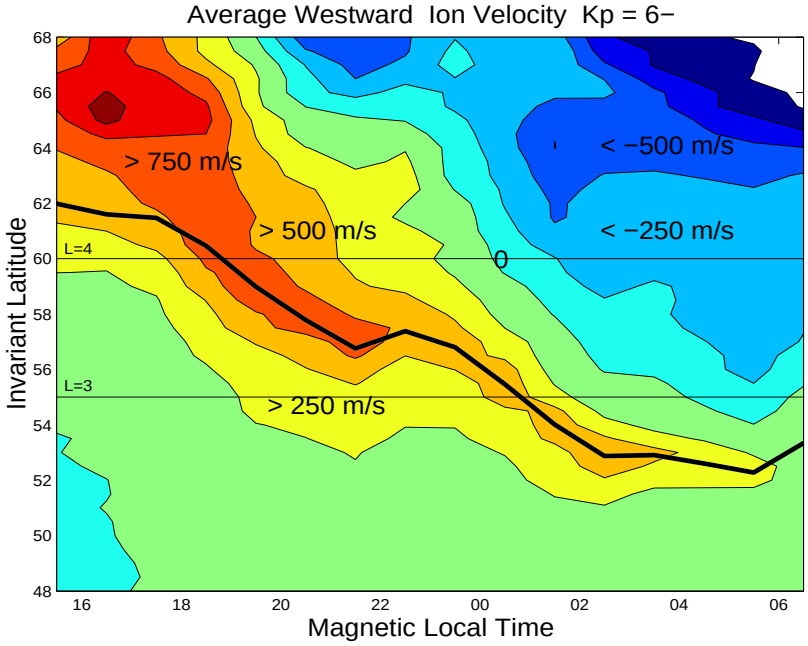

Figure 6. Bin-averaged westward ion velocity derived from Millstone Hill scans for Kp [5^+,6^0] for which SAPS has been identified. Scans at each MLT have been shifted in latitude such that the SAPS peak is aligned with the average SAPS latitude for the corresponding MLT and Kp. The heavy black curve indicates the average SAPS peak position.

of 60˚Λ (L=4) spanning midnight from 20 MLT to 04 MLT. In the dusk sector, SAPS lies at the equatorward edge of the westward two-cell auroral convection whose magnitude exceeds 1000 m/s. At and after midnight MLT, the strongest westward convection is associated with the SAPS peak, which is found equatorward of 55˚Λ (L=3) through the post-midnight sector. There is an indication in this averaged presentation of a second, more-poleward, auroral convection peak near 62˚Λ between 20 MLT and 00 MLT.

Bin-Averaged Models

The peak-picking technique described above first determines the presence of SAPS in a scan and then determines the averages of the SAPS characteristics. A second technique treats all observations equally, independent of whether or not SAPS could be identified in a scan. To investigate whether or not the SAPS phenomenon was statistically significant in the overall database, bin-averaged models of the westward convection velocity were created following the method of Foster et al. [1986]. Binned ion flow patterns were generated from the radar data for integral ranges of Kp. Data were sorted into independent bins of one hour of local time and 1.25 deg of invariant latitude between 44˚ and 70˚. Bins containing fewer than 5 data points were excluded from the pattern generation. Fully independent averages of the westward velocity were determined bin by bin.

Patterns of electrostatic potential can be generated by poleward integration of the average east-west plasma convection velocity beginning in the strict corotation region at low latitude (cf.

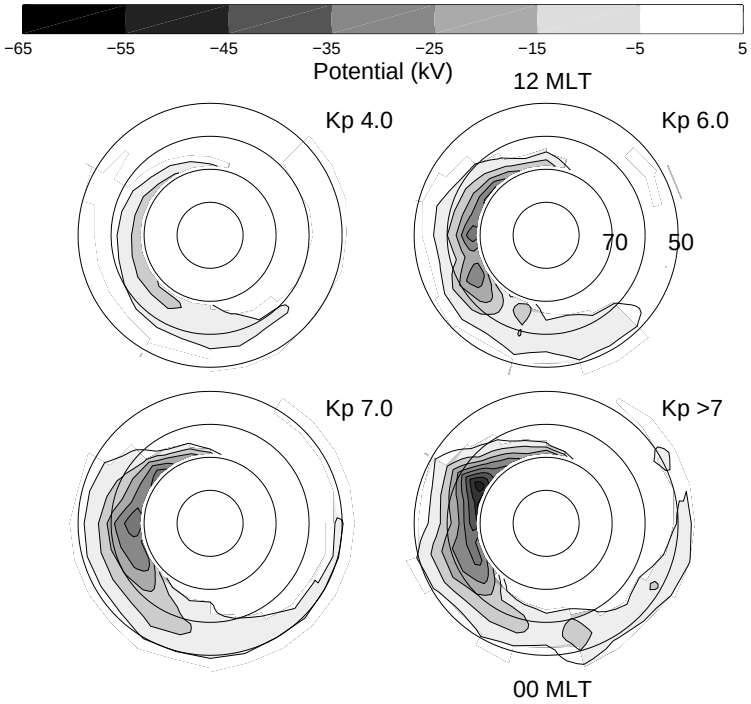

Figure 7. Patterns of negative electrostatic potential have been derived by poleward integratio of the average westward velocity across the subauroral region for four levels of the Kp index Circles are spaced at 10˚ increments of invariant latitude. Only the region of negative potentia is shown in order to emphasize its extent across the night sector between 50˚ Λ and 60˚Λ. Regions of equatorward-directed potential gradient are associated with SAPS convection. Fc Kp>6, 15kV to >30 kV of potential are associated with the SAPS in the post-midnight subau roral ionosphere.

Foster et al. [1981; 1982]). The patterns of Figure 7 were derived from our bin-averaged westward-velocity models sorted by Kp index in integral Kp steps (i.e. Kp 6 includes Kp 6– through Kp 6+). Potential patterns are displayed in co-rotating coordinates, and for emphasis in this study of SAPS, only the negative potential region is displayed and shaded. Poleward-directed electric field occurs in regions of negative (poleward) gradient of the potential and our statistical patterns indicate that such conditions span the nightside subauroral region between 50˚ and 60˚Λ and extend to near dawn MLT for high-Kp conditions. The well-organized patterns of poleward electric field and westward plasma convection at subauroral latitudes in the night sector seen in Figure 7 indicate that the SAPS convection region readily appears using standard empirical averaging techniques when sufficient subauroral data are included in the procedure We conclude that the SAPS westward velocity is a significant and repeatable feature of the overall pattern of ionospheric convection, and we stress the importance of including these subauroral electric fields in models of ring current formation and stormtime ionosphere/thermosphere dynamics.

Occurrence Statistics

The geophysical or Space Weather significance of SAPS depends on the strength and extent of its effects, and on its probability of occurrence. We have used the Millstone Hill data set to investigate occurrence probability. Investigation of each scan has determined the characteristics of all SAPS observations for each Kp and MLT over a 20-year interval. We have defined occurrence probability as the number of SAPS events divided by the total number of scans for each Kp and MLT interval. Figure 8 presents contours of the percent occurrence of SAPS in the Millstone hill database. SAPS occurrence probability is greater than 50% between 20 MLT and 02 MLT for Kp >~5. For Kp ~ 5+, the SAPS probability exceeds 80% between 20 MLT and 00 MLT. For high Kp (Kp > 6), occurrence probability is greatest near dusk (16-18 MLT). An occurrence probability >40% extends to near dawn (06 MLT) for Kp ~ 5. It is seen readily that SAPS, as described in this study, is commonly observed across the night time sector in moderate and strongly disturbed conditions.

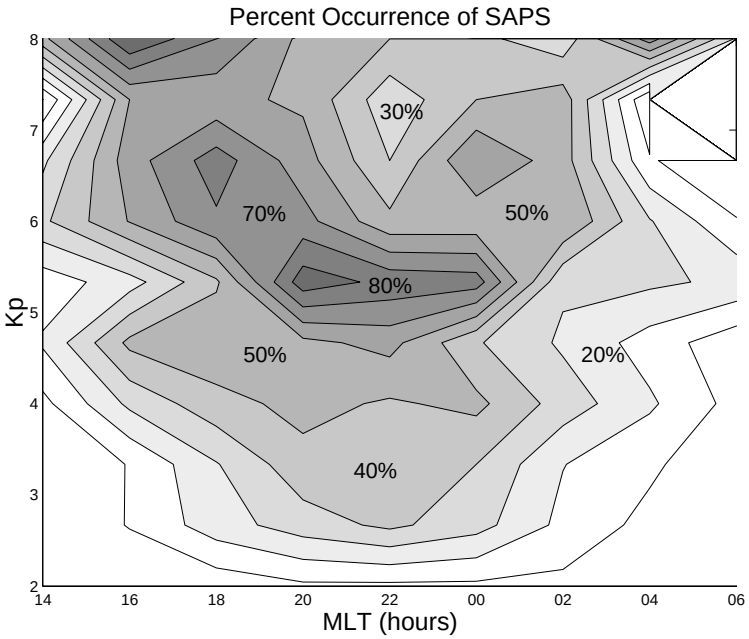

Figure 8. Occurrence probability for SAPS in the Millstone Hill database has been determined for the ~10,000 radar scans examined in this study. For Kp ~ 5+, the SAPS probability exceeds 80% near 22 MLT. For high Kp (Kp > 6), occurrence probability is greatest near dusk (16-18 MLT). An occurrence probability >40% extends to near dawn (06 MLT) for Kp ~ 5.

For a limited range of Kp we can determine the probability of SAPS occurrence as a function of latitude and MLT. Figure 9 presents such results for Kp [5^{+},6^{0}]. SAPS occurrence probability exceeds 30% in the pre-midnight sector (19 MLT - 23 MLT) near 57˚Λ, and in the post-midnight

sector near 52˚Λ. Of note is the relatively large probability of a narrow (~3˚) region of SAPS westward convection at normally mid latitudes (52˚Λ) in the early morning sector. Although the average magnitude of the SAPS in this region is not large (250-500 m/s), its effects on the redistribution of thermal plasmas and the formation of ionospheric gradients or irregularities may be significant.

Discussion

Both SAPS and SAID are associated with magnetosphere-ionosphere coupling and ionospheric feedback in the region where magnetospheric field-aligned currents (FAC) attempt to close across the subauroral ionosphere. Foster and Burke [2002] provide a brief description of this process, which is consistent with the model for SAID discussed by Anderson et al. [1993] and others. As disturbance electric fields energize ring-current particles and transport them into the inner magnetosphere, large pressure maxima develop in the nightside magnetosphere (e.g. modeling of Liemohn et al. [2001], and others). Misalignments between gradients in plasma pressure and magnetic flux tube volume cause Region 2 FACs to flow into/out of the ionosphere evening/morning sector [*Harel et al.*, 1981]. A fraction of Region 2 FACs flow into regions of low ionospheric conductivity at sub-auroral latitudes where large polarization electric fields, needed to maintain current continuity, drive rapidly drifting plasma polarization streams. Within the region of strong plasma drifts frictional heating enhances ionospheric recombination rates [*Schunk et al.,* 1976], accelerating the reduction of ionospheric conductivity in the channel. In turn, the intensity of polarization electric fields increases, leading to still deeper ionospheric troughs. Although Region 2 FACs at sub-auroral latitudes are usually small, low ambient plasma densities result in feedback which increases the polarization electric fields and decreases ionospheric conductances, enhancing the strength of the SAPS. The persistence of the SAPS events is a consequence of the long dissipation time for the ring current pressure gradients. As long as the pressure gradients exist, they drive field-aligned Region-II currents, and these give rise to the broad electric fields and significant subauroral potential found in the SAPS.

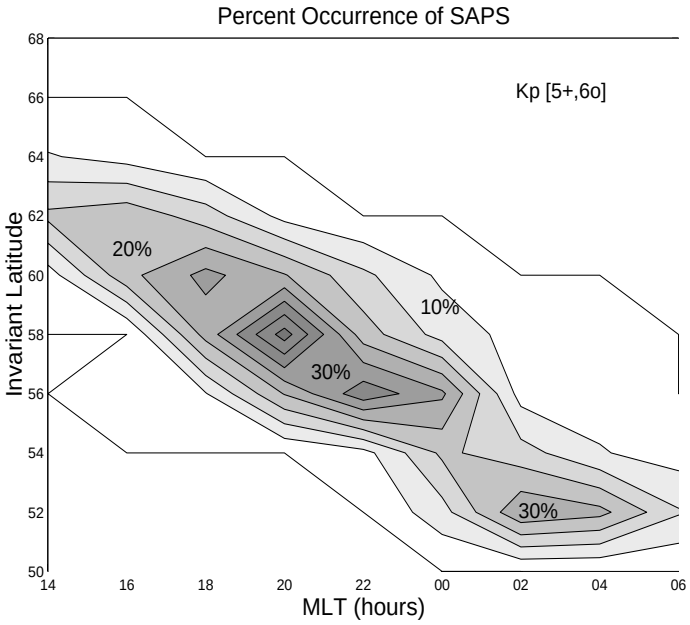

Figure 9. Occurrence probability of SAPS for Kp in the range [5^{+},6^{0}] exceeds 30% in the pre-midnight sector (19 MLT - 23 MLT) near 57˚Λ, and in the pos midnight sector near 52˚Λ.

Subauroral electric fields play critical roles in energizing and transporting ring current ions as well as convecting thermal plasma in the inner magnetosphere and in the mid to low latitude ionosphere. Subsequent studies combining ring current and plasmasphere imaging from the IMAGE satellite, radar and other ground-based observations of the development of SAPS electric fields, and inner magnetosphere modeling will investigate the important topic of ring current

development.

The subauroral polarization stream has considerable consequences on the dynamics and redistribution of thermal plasma within the coupled inner magnetosphere/ionosphere system. Anderson et al. [2001] have demonstrated that the SAID electric fields are magnetically conjugate and extend along magnetic field lines into the magnetosphere. The overlap of SAPS with the plasmasphere erodes its outer layers to form the steep disturbed-time plasmapause and spectacular plasmaspheric tails which now have been imaged with the EUV detector on the IMAGE satellite [Foster et al., 2002]. As the polarization stream sweeps sunward, entrained plasmaspheric material is seen at ionospheric altitudes as plumes of storm enhanced density [Foster, 1993], and near the dayside magnetopause as plasmaspheric drainage plumes [Su et al., 2001]. The SAPS convection channel carries storm enhanced density and patches of elevated total electron content (TEC) to mid and polar latitudes where associated density/TEC gradients and irregularities constitute significant space weather hazards [Vo and Foster, 2001].

The subauroral polarization stream, in varying levels of intensity and spatial extent, is seen as a persistent and effectively permanent feature of the disturbed nightside convection pattern. Just as the narrow SAID are associated with deep night time ionospheric troughs (e.g. Anderson et al.[1991]; Karlsson et al. [1998]), our Figure 1 and the study of Foster et al. [1994] depict how SAPS spans the low-ionospheric conductivity region between the equatorward edge of plasma sheet particle precipitation and the plasmapause. The position, extent, and intensity of the subauroral electric field and ion convection within the SAPS varies with changing activity. Pre-midnight, the SAPS westward convection lies equatorward of L=4, spans 3˚ - 5˚ of latitude, and has an average peak amplitude of 1000 m/s. In the pre-dawn sector, SAPS is seen as a region of antisunward convection equatorward of L=3, spanning ~3˚ of latitude, with an average peak amplitude of 400 m/s.

Acknowledgements: We thank J. M. Holt and members of the Haystack Observatory Atmospheric Sciences Group at the Millstone Hill Observatory for assembling and maintaining the database of radar observations which is the basis of this study, and P. J. Erickson and F. D. Lind for helpful discussions. DMSP observations presented in Figure 1 were provided by F. J. Rich. Millstone Hill observations and analysis are supported by the National Science Foundation through a Co-operative Agreement with the Massachusetts Institute of Technology.

(in press *Journal of Geophysical Research*, Sept. 2002)

References

Anderson, P. C., R. A. Heelis, and W. B. Hanson, The ionospheric signatures of rapid subauroral ion drifts, *J. Geophys. Res*., *968*, 5785, 1991.

Anderson, P. C., W. B. Hanson, R. A. Heelis, J. D. Craven, D. N. Baker, and L. A. Frank, A proposed production model of rapid sub auroral ion drifts and their relationship to substring evolution, *J. Geophys. Res*., *98*, 6069, 1993.

Anderson, P. C., D. L. Carpenter, K. Tsuruda, T. Mukai, and F. J. Rich, Multisatellite observations of rapid subauroral ion drifts (SAID), *J. Geophys. Res*., *106*, 29585, 2001.

Burke, W.J., N.C. Maynard, M.P. Hagan, R.A. Wolf, G.R. Wilson, L.C. Gentile, M.S. Gussenhoven, C.Y. Huang, T.W. Garner, and F.J. Rich, Electrodynamics of the inner magnetosphere observed in the dusk sector by CRESS and DMSP during the magnetic storm of June 4-6, 1991. *J. Geophys. Res., 103,* 29399, 1998.

Erickson, P. J., J. C. Foster, and J. M. Holt, Inferred Electric Field Variability in the polarization jet from Millstone Hill *E* Region Coherent Scatter, *Radio Sci.*, in press, 2002.

Foster, J. C., Storm-Time Plasma Transport at Middle and High Latitudes, *J. Geophys. Res., 98,* 1675-1689. 1993.

Foster, J. C., and W. J. Burke, SAPS: A new characterization for sub-auroral electric fields, *EOS, 83*, 393-394, 2002.

Foster, J. C., and F. J. Rich, Prompt midlatitude electric field effects during severe geomagnetic storms, *J. Geophys. Res*., *103,* 26367, 1998.

Foster, J. C., C. G. Park, L. H. Brace, J. R. Burrows, J. H. Hoffman, E. J. Maier, J. H. Whittaker, Plasmapause signatures in the ionosphere and magnetosphere, *J. Geophys. Res., 83,* 1175, 1978.

Foster, J. C., J. R. Doupnik and G. S. Stiles, Ionospheric Convection and Currents in the Midnight Sector on November 8, 1979, *J. Geophys. Res., 86*, 2143-2148, 1981.

Foster, J. C., P. M. Banks and J. R. Doupnik, Electrostatic potentials derived from Chatanika radar observations, *J. Geophys. Res., 87*, 7513-7524, 1982.

Foster, J. C., J. M. Holt, R. E. Musgrove, and D. S. Evans, Ionospheric Convection Associated with Discrete Levels of Particle Precipitation, *Geophys. Res. Lett., 13*, 656, 1986.

Foster, J. C., M. J. Buonsanto, M. Mendillo, D. Nottingham, F. J. Rich, and W. Denig, Coordinated Stable Auroral Red Arc Observations: Relationship to Plasma Convection, *J. Geophys. Res., 99,* 11429-11439, 1994.

Foster, J. C., A. J. Coster, P. J. Erickson, J. Goldstein, and F. J. Rich, Ionospheric Signatures of Plasmaspheric Tails, *Geophys. Res. Lett., 29*(13), 10.1029/2002GL015067, 2002.

Galperin, Y., V. N. Ponomarev, and A. G. Zosimova, Plasma convection in the polar ionosphere, *Ann. Geophys., 30*, 1, 1974.

Gonzales, C. A., M. C. Kelley, L. A. Carpenter, and R. H. Holzworth, Evidence for a magnetospheric effect on mid-latitude electric fields, *J. Geophys. Res., 83*, 4397, 1978.

Huang, C-S, J. C. Foster, and J. M. Holt, Westward Plasma Drift in the Midlatitude Ionospheric F region in the Midnight-Dawn Sector, *J. Geophys. Res.*, 106, 30349, 2001.

Karlsson, T., G. T. Marklund, L. G. Blomberg, and A. Malkki, Subauroral electric fields observed by the Freja satellite: A statistical study, *J. Geophys. Res., 103,* 4327, 1998.

Liemohn, M. W., J. U. Kozyra, C. R.Clauer, and A. J. Ridley, Computational analysis of the near-Earth magnetospheric current system during two-phase decay storms, *J. Geophys. Res., 106,* 29531, 2001.

Maynard, N. C., T. L. Aggson, and J. P. Heppner, The plasmaspheric electric field as measured by

ISEE 1, *J. Geophys. Res.*, *88*, 3991, 1983.

Ridley, A. J., and M. W. Liemohn, A model-derived stormtime asymmetric ring current driven electric field description, *J. Geophys. Res*., in press, 2002.

Rowland, D. E., and J. R. Wygant, Dependence of the large scale, inner magnetospheric electric field on geomagnetic activity, *J. Geophys. Res*., *103*, 14959, 1998.

Schunk, R. W., P. M. Banks, and W. J. Raitt, Effects of electric fields and other processes upon the nighttime high-latitude *F* layer, *J. Geophys. Res.*, *80*, 3121, 1976.

Smiddy, M., M. C. Kelley, W. Burke, F. Rich, R. Sagalyn, B. Schman, R. Hays, and S. Lai, Intense poleward-directed electric fields near the ionospheric projection of the plasmapause, *Geophys. Res. Lett.*, *4*, 543, 1977.

Spiro, R. W., R. A. Heelis, and W. B. Hanson, Rapid subauroral ion drifts observed by Atmospheric Explorer C, *Geophys. Res. Lett.*, *6*, 657-660, 1979.

Stern, D. P., The motion of a proton in the equatorial magnetosphere, *J. Geophys. Res.*, *80*, 595, 1975.

Su, Y.-J., M. F. Thomsen, J. E. Borovsky, and J. C. Foster, A linkage between polar patches and plasmaspheric drainage plumes, *Geophys. Res. Lett.*, *28*, 111-113, 2001.

Volland, H., A model of the magnetospheric electric convection field, *J. Geophys. Res.*, *83*, 2695, 1978.

Wand, R.H., and J. V. Evans, The penetration of convection electric fields to the latitude of Millstone Hill, *J. Geophys. Res.*, *86*, 5809, 1981.

Weimer, D. R., An improved model of ionospheric electric potentials including substorm perturbations and application to the Geospace Environment Modeling November 24, 1996, event, JGR, 106, 407-416, 2001.

Vasyliunas, V. M., A crude estimate of the relationship between the solar wind speed and the magnetospheric electric field, *J. Geophys. Res*., *73*, 2529, 1968.

Vo, H. B, and J. C. Foster, A Quantitative Study of Ionospheric Density Gradients at Mid-Latitudes, *J. Geophys. Res. 106*, 21555-1563, 2001.

Yeh, H.-C., J. C. Foster, F. J. Rich, and W. Swider, Storm-time electric field penetration observed at mid-latitude, *J. Geophys. Res.*, *96*, 5707, 1991.